

Cdc42 controls spindle orientation to position the apical surface during epithelial morphogenesis

Aron B. Jaffe, Noriko Kaji, Joanne Durgan, and Alan Hall

Cell Biology Program, Memorial Sloan-Kettering Cancer Center, New York, NY 10065

The establishment of apical–basal polarity within a single cell and throughout a growing tissue is a key feature of epithelial morphogenesis. To examine the underlying mechanisms, the human intestinal epithelial cell line Caco-2 was grown in a three-dimensional matrix to generate a cystlike structure, where the apical surface of each epithelial cell faces a fluid-filled central lumen. A discrete apical domain is established as early as the first cell division and between the two daughter cells. During subsequent cell divisions, the apical domain of each daughter

cell is maintained at the center of the growing structure through a combination of mitotic spindle orientation and asymmetric abscission. Depletion of Cdc42 does not prevent the establishment of apical–basal polarity in individual cells but rather disrupts spindle orientation, leading to inappropriate positioning of apical surfaces within the cyst. We conclude that Cdc42 regulates epithelial tissue morphogenesis by controlling spindle orientation during cell division.

Introduction

Cdc42 regulates the generation of cell polarity from yeast to man and in a wide range of biological contexts, and an important breakthrough in understanding the biochemical mechanisms involved came with the identification of the downstream target Par6 (Etienne-Manneville, 2004; Welchman et al., 2007). Par6 was originally identified in *Caenorhabditis elegans* as being involved in asymmetric positioning of the mitotic spindle during zygotic cell division, and subsequent work showed that Cdc42 is also required (Hung and Kemphues, 1999; Gotta et al., 2001). Other work in *C. elegans*, *Drosophila melanogaster*, and mammals has revealed a critical role for Cdc42 and Par6 in generating polarity during directed cell migration and morphogenesis (Etienne-Manneville and Hall, 2001; Hutterer et al., 2004; Na and Zernicka-Goetz, 2006; Welchman et al., 2007; Wu et al., 2007). The exact contribution of Cdc42 in these contexts is less clear. Work on directed cell migration has shown that Cdc42 acts through Par6 to control the orientation of microtubules, but Cdc42 also controls nuclear positioning and polarized actin polymerization through two other targets, MRCK (myotonic dystrophy kinase-related Cdc42-binding kinase) and p65PAK, respectively (Etienne-Manneville and Hall, 2001; Cau and Hall,

2005; Gomes et al., 2005). Cdc42 is not required for random migration, leading to the suggestion that it is not required for the establishment of polarity as such but rather to orient polarity with respect to an external cue (directional sensing; Allen et al., 1998; Srinivasan et al., 2003). A similar conclusion has emerged from experiments on Cdc42 during pheromone mating in yeast (Irazoqui et al., 2004).

Epithelial morphogenesis involves the establishment of an apical surface in an individual cell and the formation of cadherin-based adherens junctions and claudin-based tight junctions between adjacent cells. Accompanying reorganization of the actin and microtubule cytoskeletons and polarized vesicle trafficking reinforces these interactions, leading to a stable tissue of polarized cells. Expression of dominant-negative or constitutively active versions of Cdc42 in the dog kidney epithelial cell line MDCK grown on a two-dimensional surface leads to defective tight junction formation (typically a delay) as well as mislocalized delivery of basolateral proteins (Kroschewski et al., 1999; Rojas et al., 2001; Wells et al., 2006). Similar experiments performed with MDCK grown in three dimensions to provide a more physiological growth context have concluded that Cdc42 is required to form an apical surface through regulated trafficking of a vacuolar apical compartment

Correspondence to A. Hall: halla@mskcc.org

A. Jaffe's present address is Developmental and Molecular Pathways, Novartis Institutes for Biomedical Research, Cambridge, MA 02139.

Abbreviations used in this paper: aPKC, atypical PKC; CFTR, cystic fibrosis transmembrane receptor; CTX, cholera toxin; E-cadherin, epithelial cadherin.

The online version of this article contains supplemental material.

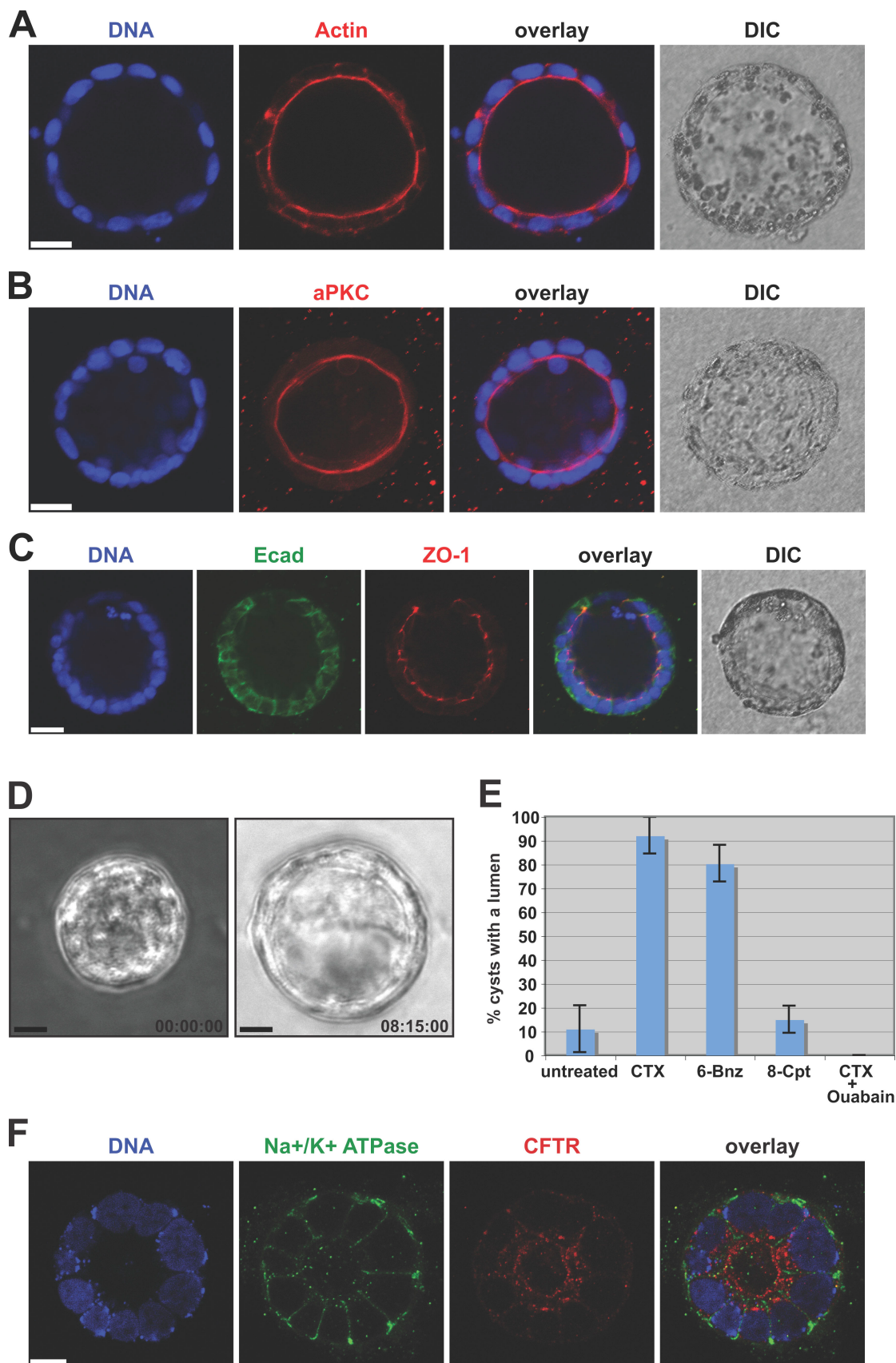


Figure 1. Caco-2 intestinal epithelial cells form polarized cysts in three dimensions. Caco-2 cells plated as a single-cell suspension in three dimensions were fixed and stained after 12 d. (A–C) Single confocal sections through the middle of cysts stained for DNA (blue) and actin (red; A); DNA (blue) and aPKC (red; B); and DNA (blue), E-cadherin (Ecad; green), and ZO-1 (red; C). Phase-contrast images (differential interference contrast [DIC]) are also shown.

(Vega-Salas et al., 1987; Martin-Belmonte et al., 2007). In this study, we describe the analysis of Caco-2, a human intestinal epithelial cell line, which, when grown in a three-dimensional matrix, generates polarized cysts with a single central lumen. We show that Cdc42 is not required for the formation of an apical surface, but instead is required to position the apical surface with respect to the growing three-dimensional structure. Our results indicate that Cdc42 regulates apical surface positioning by controlling spindle orientation during cell division.

Results and discussion

Caco-2 form fully polarized cysts in three-dimensional cultures

Caco-2 cells have been used extensively as polarized epithelial monolayers grown on two-dimensional surfaces, although few studies have been performed in three dimensions (Zhang et al., 2003; Guruswamy et al., 2008; Ivanov et al., 2008). 12 d after suspending single cells in Matrigel, Caco-2 form cysts with enhanced actin accumulation at internal surfaces facing a central lumen (Fig. 1 A). Caco-2 cysts have distinct adherens junctions (visualized by epithelial cadherin [E-cadherin] staining) and tight junctions (visualized by ZO-1 staining; Fig. 1 C), and atypical PKC (aPKC), an apical membrane marker, localizes close to the tight junctions facing the luminal space (Fig. 1 B). A three-dimensional reconstruction of a mature cyst is shown in Video 1 (available at <http://www.jcb.org/cgi/content/full/jcb.200807121/DC1>).

cAMP stimulates lumen formation through polarized expansion

Although Caco-2 grown in three dimensions form cysts, the development of a central lumen is relatively inefficient (<50%) in normal culture conditions after 12 d. However, stimulation of cAMP signaling with cholera toxin (CTX) induces dramatic and rapid lumen formation (Fig. 1 D and Video 2, available at <http://www.jcb.org/cgi/content/full/jcb.200807121/DC1>). 6 d after plating, CTX treatment results in a well-defined lumen in >90% of all Caco-2 structures in <12 h (Fig. 1 E). Time-lapse microscopy reveals that lumen formation occurs through a process of internal expansion without cell proliferation or death (Video 3). cAMP can activate PKA and Epac, an exchange factor for the small GTPase Rap1 (de Rooij et al., 1998). PKA is known to activate apical chloride channels such as the cystic fibrosis transmembrane receptor (CFTR), resulting in fluid secretion (Riordan, 2008), whereas Rap regulates epithelial morphogenesis through unknown mechanisms (Boettner and Van Aelst, 2007). To determine which pathway is involved, cAMP analogues that specifically activate PKA (6-Bnz) or Epac (8-Cpt) were used. Activation of PKA but not Epac induces lumen formation (Fig. 1 E). Recent work on intestinal development in zebrafish

concluded that lumen formation is induced through fluid accumulation driven by polarized ion transport (Bagnat et al., 2007). To examine whether Caco-2 use a similar mechanism, three-dimensional cultures were treated with CTX either alone or with ouabain, an inhibitor of the Na⁺/K⁺-ATPase pump. Ouabain completely inhibits lumen expansion (Fig. 1 F). Similar to what has previously been reported for Caco-2 cells grown in two dimensions, the CFTR chloride channel and the Na⁺/K⁺-ATPase are localized apically and laterally, respectively, in three dimensions (Fig. 1 F). These data indicate that lumen expansion occurs by ion transport–driven fluid flow. Polarized secretion (fluid or protein) to drive the separation of two opposing apical surfaces is emerging as an evolutionarily conserved mechanism for lumen formation in a wide range of epithelial tissues such as the *Drosophila* retina and trachea (Husain et al., 2006; Tsarouhas et al., 2007), the zebrafish gut (Bagnat et al., 2007), and the zebrafish neural tube (Lowery and Sive, 2005).

Cdc42 depletion inhibits Caco-2 morphogenesis

To determine the role of Cdc42 in cyst development, Caco-2 cells were transfected with nonspecific or Cdc42-specific siRNAs 1 d before plating in Matrigel (Fig. 2 B). Treatment with CTX 6 d later results in the swelling of a single central lumen in control structures, whereas 50% of Cdc42 siRNA–transfected structures appear abnormal (Fig. 2 A and Video 4, available at <http://www.jcb.org/cgi/content/full/jcb.200807121/DC1>). Immunofluorescence reveals that depletion of Cdc42 results in cysts containing multiple lumens (Fig. 2, C–E). Interestingly, the surface of each lumen within the three-dimensional structure is positive for the apical marker aPKC (Fig. 2 D) and the tight junction protein ZO-1 (Fig. 2 E). These data suggest that Cdc42 is not required for the formation of apical–basal polarity and tight junctions during Caco-2 morphogenesis but rather for the correct positioning of the apical surface with respect to the growing structure.

An apical surface is specified at the first cell division and is maintained at the center of the developing cyst by mitotic spindle positioning

To understand the mechanism by which Cdc42 depletion results in multiple lumens, the development of control Caco-2 cysts was examined. Surprisingly, an apical surface is clearly visible at the two-cell stage, as revealed by ZO-1 and aPKC localization (Fig. 3, A and B [second row]). E-cadherin is basolateral and does not overlap with ZO-1 (Fig. 3 A and Video 5, available at <http://www.jcb.org/cgi/content/full/jcb.200807121/DC1>) such that the membrane interface between two daughter cells is already demarcated into a lateral surface surrounding an

(D) Caco-2 plated as a single-cell suspension in three dimensions were cultured for 7 d and treated with 0.1 µg/ml CTX. Individual images shown from Video 2 (available at <http://www.jcb.org/cgi/content/full/jcb.200807121/DC1>) were taken at the indicated time points. (E) Lumen expansion in Caco-2 cells cultured as in D were treated with 0.1 µg/ml CTX, 100 nM of the PKA agonist 6-Bnz, 100 nM of the Epac agonist 8-Cpt, or 0.1 µg/ml CTX + 10 µM ouabain. Shown is the mean ± standard deviation for three independent experiments (50 cysts each). (F) Caco-2 was cultured for 10 d in three dimensions, fixed, and stained for DNA (blue), Na⁺/K⁺-ATPase (green), or CFTR (red). A single confocal section through the middle of the cyst is shown. Bars: (A–C) 25 µm; (D and F) 10 µm.

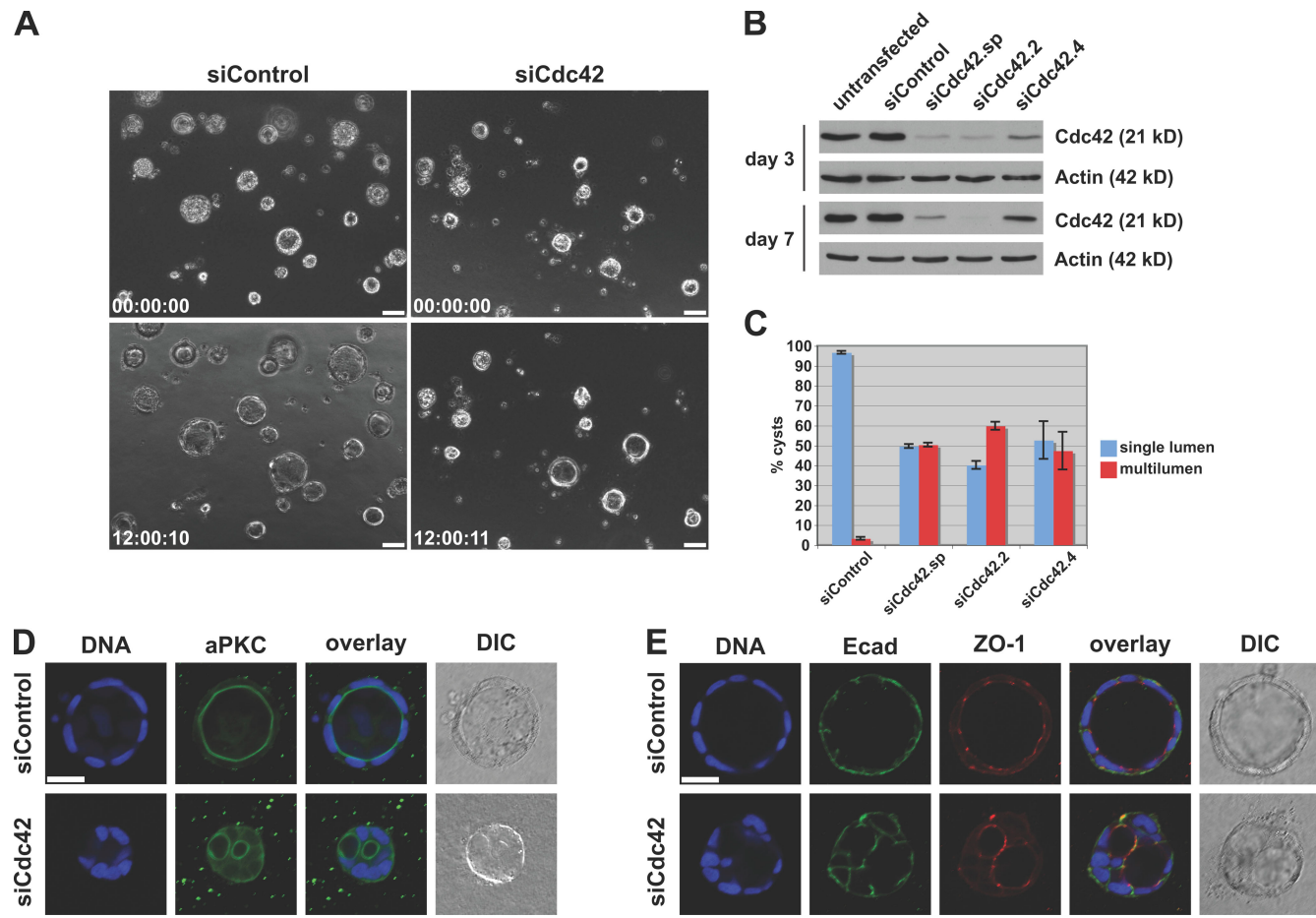


Figure 2. Cdc42 depletion induces multiple lumens. (A) Caco-2 was transfected with control or Cdc42 siRNA, plated in three dimensions, and treated with CTX at day 6 to induce luminal swelling. Phase images from cysts before (0 h) and after (12 h) treatment are shown. Note that about half of the Cdc42-depleted cysts lack a single central lumen. Bars, 50 µm. (B) Western blot of Caco-2 transfected with control siRNA, Cdc42 siRNA SMARTpool, or two different individual duplexes. Cdc42 levels are significantly reduced by 3 d and remain reduced for 7 d. (C) Caco-2 cultured as in A was fixed and stained with rhodamine phalloidin. Cysts were examined for single lumen (blue) or multiple lumens (red). The mean \pm standard deviation for three independent experiments (at least 50 cysts each) is shown. (D and E) Caco-2 cultured as in A was fixed and stained for DNA (blue) and aPKC (green; D) or DNA (blue), E-cadherin (Ecad; green), and ZO-1 (red; E). Single confocal sections through the middle of the cysts are shown. DIC, differential interference contrast. Bars, 25 µm.

apical patch. Because aPKC is delocalized around the cell periphery in single cells (Fig. 3 B, top), this suggests the apical patch is laid down during cell division, most likely cytokinesis.

As Caco-2 cells further proliferate, the apical region is maintained and localized exclusively at the center of the growing structure (Fig. 3 B, bottom three rows). This suggests that as cells divide, the mitotic spindle is oriented to give rise to two daughter cells that maintain an epithelial monolayer in a spherical structure. As shown in Fig. 3 C, this is indeed the case. This orientation of the mitotic spindle, to produce an apical–basal cleavage plane, has been seen in monolayer cultures (Reinsch and Karsenti, 1994) and *in vivo* in the mouse intestine (Fleming et al., 2007). It provides a simple mechanism for maintaining the integrity of apical membrane structures during cell division.

Cdc42 is required for mitotic spindle orientation

Based on this analysis, a consequence of Cdc42 depletion could be disruption of spindle orientation. To examine this, Caco-2 cells were transfected with Cdc42 siRNA and grown in three

dimensions. 3 d later (4 d after transfection), structures were examined for orientation of mitotic spindles (calculated as described in Fig. 4 A). Depletion of Cdc42 has a dramatic effect on spindle orientation. In control cysts, the majority of spindles are oriented perpendicular to the centroid of the cyst (mean angle = $72.3 \pm 3.9^\circ$; Fig. 4, B and C [top]). However, after Cdc42 depletion, spindle orientation is randomized (mean angle = $41.2 \pm 5.2^\circ$ and $41.8 \pm 5.7^\circ$ for duplex 2 and duplex 4, respectively; Fig. 4, B and C [bottom]), with some spindles oriented so as to produce a daughter cell in the middle of the structure (Fig. 4 D).

If the apical surface is generated between daughter cells (Fig. 3 A), the consequence of spindle misalignment will be the formation of apical patches at aberrant sites. To examine this, the localization of the apical marker aPKC was determined early in the development of Cdc42-depleted cysts. Fig. 4 E (arrows) shows that some cells have multiple distinct apical patches on their surface. These results suggest that loss of Cdc42 causes misoriented division, giving rise to an inappropriately placed apical membrane, which after expansion leads to multiple lumen.

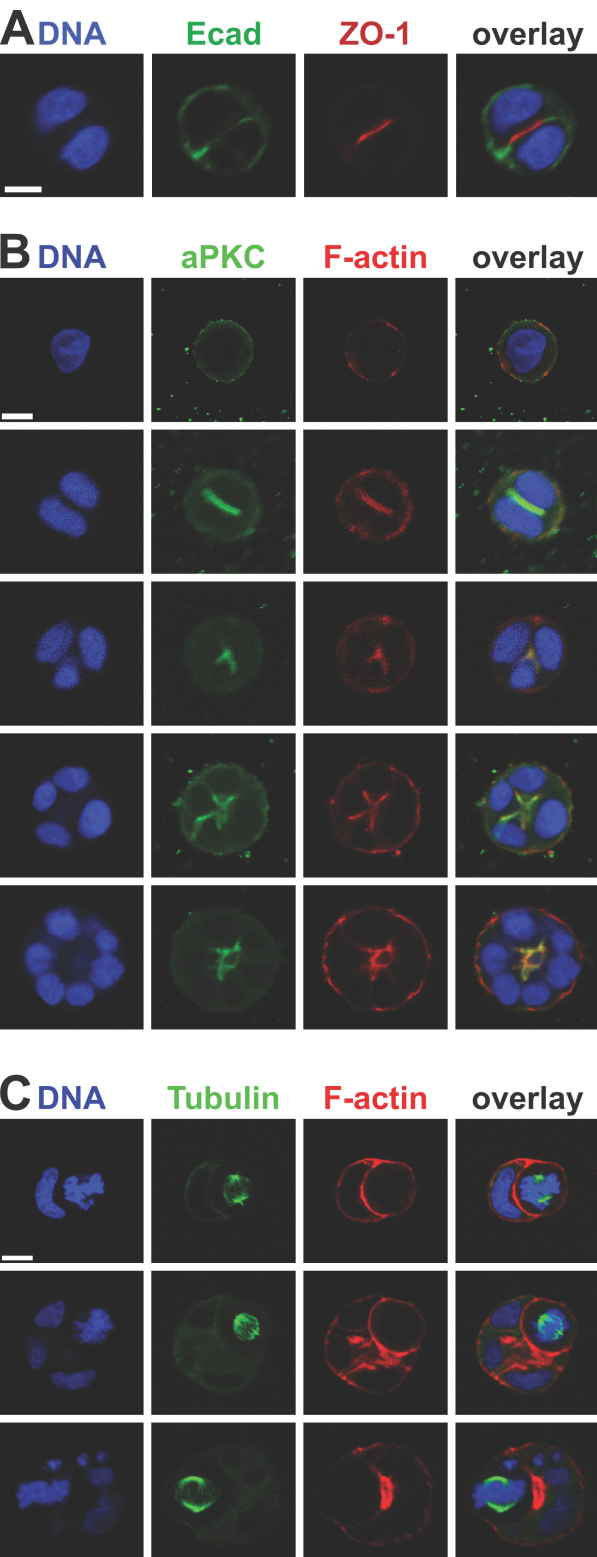


Figure 3. The apical surface is established at the first cell division and maintained at the center of the growing structure. Cells were plated as a single-cell suspension in three dimensions, fixed, stained, and analyzed by confocal microscopy. (A) A two-cell structure stained for DNA (blue), E-cadherin (Ecad; green), and ZO-1 (red). A three-dimensional reconstruction of the structure is shown in Video 5 (available at <http://www.jcb.org/cgi/content/full/jcb.200807121/DC1>). Note that apical and basolateral membrane domains (defined by ZO-1 and E-cadherin, respectively) are segregated and readily visible. (B) Caco-2 structures at different stages of

Asymmetric abscission ensures correct positioning of apical surfaces at the center of the cyst

The analysis of MDCK in two-dimensional and mouse intestinal epithelial cells *in vivo* has revealed that invagination of the cleavage furrow is asymmetric, proceeding basal to apical such that abscission occurs at the most apical point between two daughter cells (Reinsch and Karsenti, 1994; Fleming et al., 2007). This, in combination with mitotic spindle orientation, would explain the persistence of apical surfaces at the center of growing Caco-2 structures (Fig. 3 B). To examine the abscission site in Caco-2 cells, the cytokinesis midbody was visualized with a tubulin antibody. As seen in Fig. 5 A (top), at the end of the first cell division, the apical marker aPKC is associated with the midbody at the center of the interface between the two emerging daughter cells. This strongly supports the idea that the apical surface is laid down during cytokinesis, although in the case of the first cell division, abscission appears to be symmetric. In multicellular structures (Fig. 5, A [middle] and B), 91% of midbodies are located in the center of the developing cyst, suggesting that after the first cell division, all subsequent abscissions occur asymmetrically and close to the existing apical membrane (i.e., in the center of the growing structure). In Cdc42-depleted Caco-2, <40% of midbodies are located centrally, reflecting the numerous noncentrally located apical surfaces (Fig. 5, A [bottom] and B). We conclude that the loss of Cdc42 results in spindle misorientation, leading to inappropriately placed abscission sites. Because the abscission site establishes the apical surface (Fig. 5 A, midbody position), loss of Cdc42 results in the formation of multiple lumens.

Three-dimensional culture models recapitulate many of the features of *in vivo* epithelial architecture. Two cell types have been used extensively in this context: the dog kidney cell line MDCK and the human mammary epithelial cell line MCF10A. Both generate cystlike structures, but MCF10A achieve this through clearing internal cells by apoptosis and autophagy, whereas MDCK use a combination of exocytosis of intracellular vacuoles (the vacuolar apical compartment) and apoptosis of interior cells (Martin-Belmonte et al., 2007). In this study, we show that Caco-2 cysts form by polarized fluid filling in a manner similar to gut and neural tube development in zebrafish (Bagnat et al., 2007). We believe that the similarities between Caco-2 cyst formation *in vitro* and intestinal epithelia *in vivo* make this a relevant system for studying morphogenesis.

A striking observation is that Caco-2 cells display a distinct apical membrane patch as early as the two-cell stage. This appears to be linked to cytokinesis because the apical marker aPKC associates with the midbody before abscission occurs.

development were stained for DNA (blue), aPKC (green), and filamentous actin (F-actin; red). Note that single cells (top) are unpolarized in three dimensions, whereas apical polarity is readily observed in the two-cell structure (second row). (C) Caco-2 structures at different stages of development stained for DNA (blue), tubulin (green), and filamentous actin (red). Note that the mitotic spindle is oriented to produce daughter cells that preserve the spherical monolayered structure of the cyst. (A–C) Single confocal sections through the middle of each structure are shown. Bars, 10 μ m.

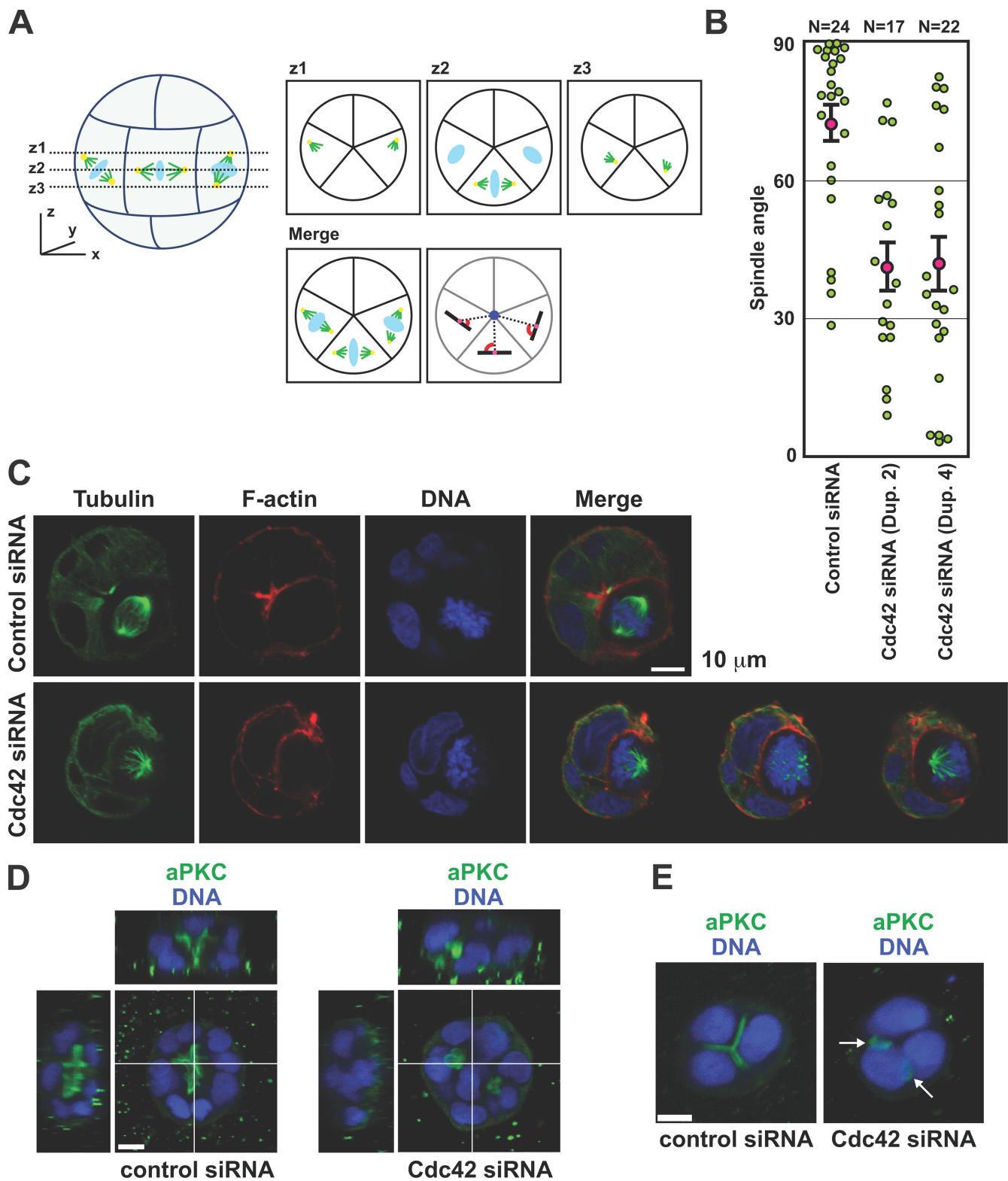


Figure 4. Cdc42 depletion disrupts mitotic spindle orientation. (A) Diagram depicting spindle angle measurement. The centroid of the cyst (dark blue circle) and the center of the spindle axis (pink circles) of a metaphase cell were drawn using ImageJ. The angle (red) between the spindle axis (black lines) and the line connecting the centroid of the cyst to the center of the spindle (dashed lines) was determined. To analyze spindle poles in different z sections, three z sections were taken so as to include both spindle poles and were merged as shown. Three schematic spindles are shown. The right and middle spindle examples represent correctly oriented spindles whose poles are positioned in one section (z2; middle spindle) or in different sections (z1 and z3; right spindle). The left spindle represents a misoriented spindle whose poles are in different z sections. Spindle microtubules, green; centrosomes, yellow; DNA, light blue. (B) Scatter diagram of metaphase spindle angles in cysts that were transfected with control or two Cdc42 siRNA duplexes from three independent experiments. Pink circles indicate mean values, green circles indicate individual data points, and error bars represent the SEM of the total number of spindles analyzed (N). (C) Caco-2 was transfected with control or Cdc42 siRNA and was fixed and stained for DNA (blue), tubulin (green),

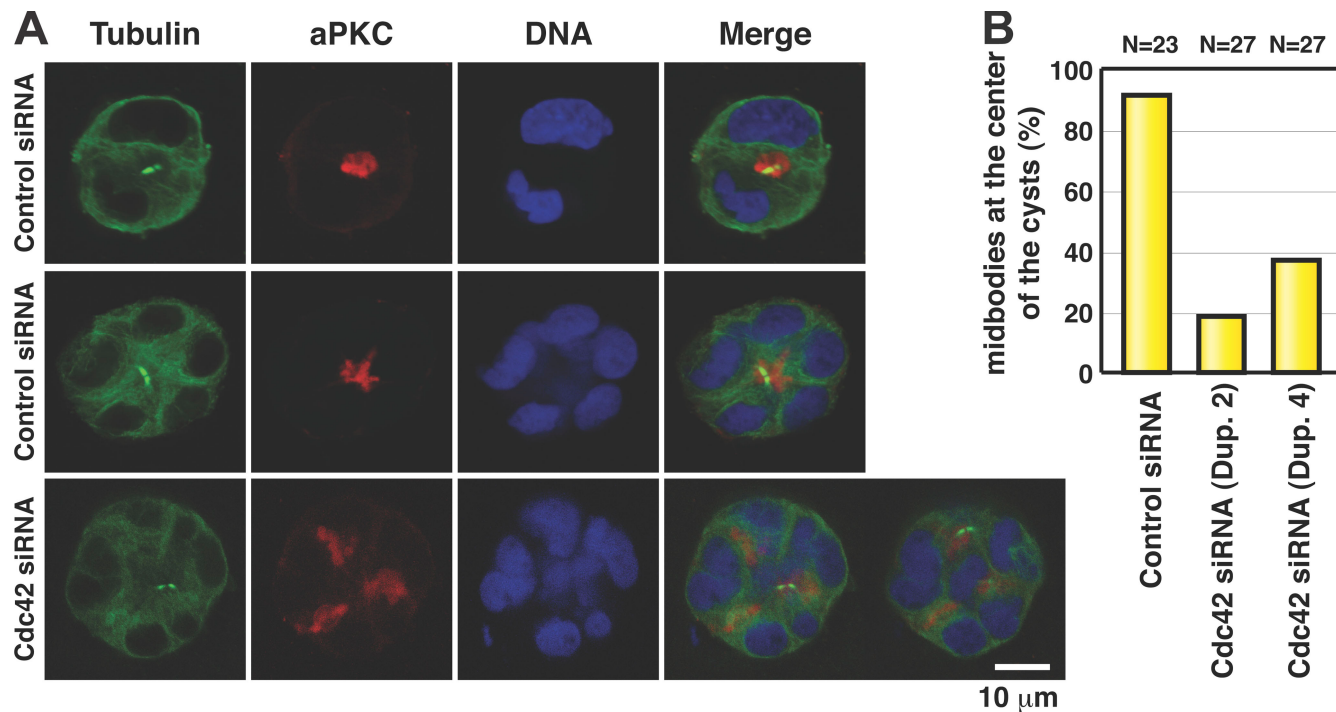


Figure 5. The midbody positions the apical surface during cyst development. (A) Caco-2 transfected with control or Cdc42 siRNA was fixed and stained for DNA (blue), tubulin (green), and aPKC (red). (top) A control cyst at the two-cell stage (note that abscission appears to have occurred symmetrically). (middle) A larger control cyst, with the midbody in the center of the developing structure (apical region of dividing cell) reflecting asymmetric abscission. (bottom) Cdc42 siRNA structure with one midbody positioned normally at the center and another midbody (located in a different z section) abnormally positioned. (B) Quantitation of midbodies at the center of the cyst from three independent experiments. The total number of midbodies is indicated (N). A midbody is regarded as being in the center if it is located at a distance from the centroid that is less than one third the radius of the structure.

Apical surfaces are maintained at the center of the growing Caco-2 structure during subsequent cell divisions through a combination of (a) orientation of the mitotic spindle to generate radial cleavage and (b) asymmetric positioning of the midbody to generate apical abscission (Fig. S1 A, available at <http://www.jcb.org/cgi/content/full/jcb.200807121/DC1>). Oriented cell division coupled to apical abscission provides a mechanism for maintaining the structural integrity of an epithelial barrier in tissues undergoing continuous proliferation such as the intestine (Reinsch and Karsenti, 1994; Fleming et al., 2007).

Cdc42 depletion in MDCK cells leads to an accumulation of intracellular vesicles containing apical proteins, resulting in intracellular lumens, as well as cells in the middle of the cyst that are eventually cleared by apoptosis, resulting in intercellular lumens (Martin-Belmonte et al., 2007). We find no evidence for cell death after depleting Cdc42 in Caco-2; instead, multiple intercellular lumens are formed, each of which appears to be correctly polarized as judged by aPKC and tight junction localization. Because these ectopic lumens expand through polarized fluid secretion, this provides further evidence for appropriate apical–basal polarity. Further analysis reveals that Cdc42 deple-

tion causes spindle misorientation, leading to disruption of cleavage furrow orientation and mislocalization of the midbody during cytokinesis. Because the apical surface is established at the site of abscission, Cdc42 depletion results in noncentrally located apical surfaces to generate ectopic lumens (Fig. S1 B). Cdc42 has been reported to control spindle orientation in the early *C. elegans* embryo and in mouse oocytes, and this is linked to its association with Par6 (Gotta et al., 2001; Na and Zernicka-Goetz, 2006), but other potential Cdc42 targets have also been linked to spindle orientation, including LIM kinase and phosphatidylinositol 3-kinase (Toyoshima et al., 2007; Kaji et al., 2008). Finally, it is interesting to note that the loss of asymmetric abscission (Fig. S1 C) could in itself lead to an inappropriately positioned apical surface. The mechanisms controlling apical midbody positioning are not well understood. Recent work on zygotic cell division in *C. elegans* has implicated septins and anillin (Maddox et al., 2007), and interestingly, the former has been linked to Cdc42 through the Borg family, and the latter is a target of Rho (Piekny and Glotzer, 2008). We are currently using live cell imaging to characterize in more detail the specific roles of Cdc42 in this morphogenetic process.

and filamentous actin (F-actin; red). Single confocal sections through the center of the cysts are shown. Three z sections are shown for the Cdc42 siRNA cyst to reveal both poles of the misoriented spindle. (D and E) Caco-2 transfected with control or Cdc42 siRNA was fixed and stained for DNA (blue) and aPKC (green). (D) Cdc42 siRNA structures contain cells in the middle, with apical domains present between inner and outer cells. (E) Cdc42 siRNA structures possess apical domains that are not in the center and single cells with more than one apical domain. Arrows indicate cells with multiple distinct apical patches on their surface. Bars, 10 μm.

Materials and methods

Reagents

Cell culture medium was obtained from Invitrogen or an in-house facility. Primary antibodies used in this study were Cdc42 (mouse monoclonal clone 44; BD), β -actin (clone AC-74; Sigma-Aldrich), Flag (clone M2; Sigma-Aldrich), α -tubulin (clone DM1A; Sigma-Aldrich), rat anti-E-cadherin (clone ECCD-2; Invitrogen), rabbit polyclonal PKC ζ (C-20; Santa Cruz Biotechnology, Inc.), ZO-1 (Invitrogen), and CFTR (NBD-R; provided by A.P. Naren, University of Tennessee, Knoxville, TN). The $\alpha 5$ monoclonal antibody to Na $^+$ /K $^+$ -ATPase developed by D.M. Fambrough was obtained from the Developmental Studies Hybridoma Bank and maintained by the University of Iowa. Alexa Fluor 488 and 568 secondary antibodies, rhodamine-conjugated phalloidin, and Prolong gold antifade with DAPI were obtained from Invitrogen. HRP-conjugated secondary antibodies were obtained from Dako, and DRAQ5 and 8-Cpt-2'-O-Me-cAMP sodium salt were obtained from Axxora LLC. N(6)-benzoyl-cAMP sodium salt was obtained from EMD, and other chemicals were obtained from Sigma-Aldrich.

Cell culture

Caco-2 cells were cultured in Dulbecco's modified Eagle's medium supplemented with 10% fetal calf serum and penicillin-streptomycin (100 IU/ml and 100 mg/ml, respectively) at 37°C in 5% CO $_2$. To produce cysts, Caco-2 cells were plated either on top of matrix (for time lapse) or embedded in matrix (for immunofluorescence). For on-top cultures, cells were trypsinized and resuspended (10^4 cells/ml) in media plus 2% Matrigel (BD). 400 μ l of suspension was plated in each well of an 8-well chamber slide (BD) precoated with 30 μ l of Matrigel. For embedded cultures, cells were trypsinized and mixed with Hepes (final concentration of 0.02 M), collagen I (final concentration of 1 mg/ml; Trevigen), and Matrigel (final concentration of 40%) to 6×10^4 cells/ml. Approximately 100 μ l was plated in each well of an 8-well chamber slide, allowed to solidify for 30 min, and overlayed with 400 μ l of media.

Microscopy

Immunofluorescence of embedded Caco-2 cysts was performed as described previously for MCF10A cysts (Debnath et al., 2003) with the following modifications. Before blocking, Caco-2 chambers were rinsed with PBS and treated with 100 μ l of 50 U/ml collagenase-1 (Sigma-Aldrich) in PBS for 15 min at room temperature. After incubation with fluorescence-conjugated secondary antibodies, DNA was stained with a 1:300 dilution of DRAQ5 and mounted in Prolong gold antifade. Confocal microscopy was performed at room temperature on a microscope (TCS SP2 AOBS; Leica) using a plan Apo 20 \times 0.7 NA dry differential interference contrast C objective (HC; Leica) and 2.29 \times zoom or on a microscope (TCS SP2; Leica) using a plan Apo 63 \times 1.32–0.6 oil CS objective (HXC; Leica) and 2 or 4 \times zoom. Images were collected with confocal software (Leica). Scale bars were added, and images were processed using Volocity (PerkinElmer). Video 1 was generated with Amira 4 (Visage Imaging). For time-lapse video microscopy, Caco-2 cysts were grown on top, treated as indicated in the text, and imaged at 37°C with a plan Neofluar 10 \times 0.3 NA Ph1 objective (EC; Carl Zeiss, Inc.) on a microscope (Axiovert 200; Carl Zeiss, Inc.) equipped with a motorized stage and a camera (Orca-ER-1394; Hamamatsu Photonics) controlled by Axiovision software (Carl Zeiss, Inc.). Images of two fields per well were taken every 5 min for the indicated time period. Annotations (time stamp and scale bar) were added using Axiovision software, exported as tiff files, and assembled into videos with MetaMorph (MDS Analytical Technologies).

Measurement of spindle angle

To measure spindle angles (see Fig. 4 A for schematic), confocal images of metaphase cells in the middle region of the cysts were collected, and the centroid of the cyst (Fig. 4 A, dark blue circle) and center of the spindle axis (Fig. 4 A, pink circles) were drawn using ImageJ (National Institutes of Health). The angle (Fig. 4 A, red) between the spindle axis (Fig. 4 A, black lines) and the line connecting the centroid of the cyst and the center of the spindle (Fig. 4 A, dashed lines) was analyzed. When both spindle poles were not in one z section, three z sections including each spindle pole were taken and merged to draw a line of spindle axis.

RNAi

To deplete Cdc42, a SMARTpool (a mixture of four siRNA duplexes) and individual siRNA duplexes were purchased from Thermo Fisher Scientific. For siRNA transfections, 0.5×10^5 Caco-2 cells were plated into a well of a 6-well plate, and the next day 100 pmol of siRNA duplex was trans-

fected using Dharmafect 1 (Thermo Fisher Scientific) according to the manufacturer's specifications. Under these conditions, 70–90% of transfection efficiency was achieved as judged by siGloGreen control (Thermo Fisher Scientific). To analyze the knockdown efficiency, cells were replated onto 6-cm plates 24 h after transfection and harvested for Western blotting on the day indicated. For three-dimensional cultures, cells were plated in matrix 24 h after transfection and analyzed as indicated.

Western blotting

Cells were washed with cold PBS and lysed in radio immunoprecipitation assay buffer (50 mM Tris-HCl, pH 8, 150 mM NaCl, 1% NP-40, 0.5% sodium deoxycholate, and 0.1% SDS). Cell debris was removed by centrifugation at 14,000 rpm for 10 min at 4°C. SDS sample buffer was added to equal amounts of lysate, resolved by SDS-PAGE, blotted onto nitrocellulose membranes, and analyzed with the antibodies indicated in the text.

Online supplemental material

Fig. S1 schematically depicts Caco-2 three-dimensional morphogenesis and the effects of Cdc42 depletion. Video 1 shows a three-dimensional reconstruction of a Caco-2 cyst. Video 2 shows a Caco-2 cyst treated with CTX. Video 3 is similar to Video 2, except it shows prolonged treatment with CTX at a lower magnification. Video 4 shows siRNA Cdc42-transfected Caco-2 cysts treated with CTX. Video 5 shows a three-dimensional reconstruction of a two-cell stage Caco-2 structure stained for DNA, E-cadherin, and ZO-1. Online supplemental material is available at <http://www.jcb.org/cgi/content/full/jcb.200807121/DC1>.

We thank the Sloan-Kettering Institute Molecular Cytology Core Facility (K. Manova-Todorova, T. Tong, Y. Romin, and Z. Lazar) for help with imaging, Dr. A.P. Naren for CFTR antibodies, and the Hall laboratory for helpful discussions.

This work was supported by a National Institutes of Health grant (GM081435) to A. Hall, a National Cancer Institute core center grant (P30-CA 08748), and by the Alan and Sandra Gerry Metastasis Research Initiative. N. Kaji is supported by the Uehara Memorial Foundation, and J. Durgan is a Charles H. Revson Foundation Senior Fellow in Biomedical Sciences.

Submitted: 22 July 2008

Accepted: 1 October 2008

References

- Allen, W.E., D. Zicha, A.J. Ridley, and G.E. Jones. 1998. A role for Cdc42 in macrophage chemotaxis. *J. Cell Biol.* 141:1147–1157.
- Bagnat, M., I.D. Cheung, K.E. Mostov, and D.Y. Stainier. 2007. Genetic control of single lumen formation in the zebrafish gut. *Nat. Cell Biol.* 9:954–960.
- Boettner, B., and L. Van Aelst. 2007. The Rap GTPase activator *Drosophila* PDZ-GEF regulates cell shape in epithelial migration and morphogenesis. *Mol. Cell. Biol.* 27:7966–7980.
- Cau, J., and A. Hall. 2005. Cdc42 controls the polarity of the actin and microtubule cytoskeletons through two distinct signal transduction pathways. *J. Cell Sci.* 118:2579–2587.
- de Rooij, J., F. Zwartkruis, M.H. Verheijen, R.H. Cool, S.M. Nijman, A. Wittinghofer, and J.L. Bos. 1998. Epac is a Rap1 guanine-nucleotide-exchange factor directly activated by cyclic AMP. *Nature*. 396:474–477.
- Debnath, J., S.K. Muthuswamy, and J.S. Brugge. 2003. Morphogenesis and oncogenesis of MCF-10A mammary epithelial acini grown in three-dimensional basement membrane cultures. *Methods*. 30:256–268.
- Etienne-Manneville, S. 2004. Cdc42—the centre of polarity. *J. Cell Sci.* 117:1291–1300.
- Etienne-Manneville, S., and A. Hall. 2001. Integrin-mediated activation of Cdc42 controls cell polarity in migrating astrocytes through PKC ζ . *Cell*. 106:489–498.
- Fleming, E.S., M. Zajac, D.M. Moschenross, D.C. Montrose, D.W. Rosenberg, A.E. Cowan, and J.S. Tirnauer. 2007. Planar spindle orientation and asymmetric cytokinesis in the mouse small intestine. *J. Histochem. Cytochem.* 55:1173–1180.
- Gomes, E.R., S. Jani, and G.G. Gunderson. 2005. Nuclear movement regulated by Cdc42, MRCK, myosin, and actin flow establishes MTOC polarization in migrating cells. *Cell*. 121:451–463.
- Gotta, M., M.C. Abraham, and J. Ahringer. 2001. CDC-42 controls early cell polarity and spindle orientation in *C. elegans*. *Curr. Biol.* 11:482–488.
- Guruswamy, S., M.V. Swamy, C.I. Choi, V.E. Steele, and C.V. Rao. 2008. S-adenosyl L-methionine inhibits azoxymethane-induced colonic aberrant crypt foci in F344 rats and suppresses human colon cancer Caco-2 cell growth in 3D culture. *Int. J. Cancer*. 122:25–30.

- Hung, T.J., and K.J. Kemphues. 1999. PAR-6 is a conserved PDZ domain-containing protein that colocalizes with PAR-3 in *Caenorhabditis elegans* embryos. *Development*. 126:127–135.
- Husain, N., M. Pellikka, H. Hong, T. Klimentova, K.M. Choe, T.R. Clandinin, and U. Tepass. 2006. The agrin/perlecan-related protein eyes shut is essential for epithelial lumen formation in the *Drosophila* retina. *Dev. Cell*. 11:483–493.
- Hutterer, A., J. Betschinger, M. Petronczki, and J.A. Knoblich. 2004. Sequential roles of Cdc42, Par-6, aPKC, and Lgl in the establishment of epithelial polarity during *Drosophila* embryogenesis. *Dev. Cell*. 6:845–854.
- Irazoqui, J.E., A.S. Gladfelter, and D.J. Lew. 2004. Cdc42p, GTP hydrolysis, and the cell's sense of direction. *Cell Cycle*. 3:861–864.
- Ivanov, A.I., A.M. Hopkins, G. Brown, K. Gerner-Smidt, B. Babbin, C.A. Parkos, and A. Nusrat. 2008. Myosin II regulates the shape of three-dimensional intestinal epithelial cysts. *J. Cell Sci.* 121:1803–1814.
- Kaji, N., A. Muramoto, and K. Mizuno. 2008. LIM kinase-mediated cofilin phosphorylation during mitosis is required for precise spindle positioning. *J. Biol. Chem.* 283:4983–4992.
- Kroschewski, R., A. Hall, and I. Mellman. 1999. Cdc42 controls secretory and endocytic transport to the basolateral plasma membrane of MDCK cells. *Nat. Cell Biol.* 1:8–13.
- Lowery, L.A., and H. Sive. 2005. Initial formation of zebrafish brain ventricles occurs independently of circulation and requires the nagie oko and snake-head/atp1a1a1 gene products. *Development*. 132:2057–2067.
- Maddox, A.S., L. Lewellyn, A. Desai, and K. Oegema. 2007. Anillin and the septins promote asymmetric ingression of the cytokinetic furrow. *Dev. Cell*. 12:827–835.
- Martin-Belmonte, F., A. Gassama, A. Datta, W. Yu, U. Rescher, V. Gerke, and K. Mostov. 2007. PTEN-mediated apical segregation of phosphoinositides controls epithelial morphogenesis through Cdc42. *Cell*. 128:383–397.
- Na, J., and M. Zernicka-Goetz. 2006. Asymmetric positioning and organization of the meiotic spindle of mouse oocytes requires CDC42 function. *Curr. Biol.* 16:1249–1254.
- Piekny, A.J., and M. Glotzer. 2008. Anillin is a scaffold protein that links RhoA, actin, and myosin during cytokinesis. *Curr. Biol.* 18:30–36.
- Reinsch, S., and E. Karsenti. 1994. Orientation of spindle axis and distribution of plasma membrane proteins during cell division in polarized MDCKII cells. *J. Cell Biol.* 126:1509–1526.
- Riordan, J.R. 2008. CFTR function and prospects for therapy. *Annu. Rev. Biochem.* 77:701–726.
- Rojas, R., W.G. Ruiz, S.M. Leung, T.S. Jou, and G. Apodaca. 2001. Cdc42-dependent modulation of tight junctions and membrane protein traffic in polarized Madin-Darby canine kidney cells. *Mol. Biol. Cell*. 12:2257–2274.
- Srinivasan, S., F. Wang, S. Glavas, A. Ott, F. Hofmann, K. Aktories, D. Kalman, and H.R. Bourne. 2003. Rac and Cdc42 play distinct roles in regulating PI(3,4,5)P3 and polarity during neutrophil chemotaxis. *J. Cell Biol.* 160:375–385.
- Toyoshima, F., S. Matsumura, H. Morimoto, M. Mitsushima, and E. Nishida. 2007. PtdIns(3,4,5)P3 regulates spindle orientation in adherent cells. *Dev. Cell*. 13:796–811.
- Tsarouhas, V., K.A. Senti, S.A. Jayaram, K. Tiklova, J. Hemphala, J. Adler, and C. Samakovlis. 2007. Sequential pulses of apical epithelial secretion and endocytosis drive airway maturation in *Drosophila*. *Dev. Cell*. 13:214–225.
- Vega-Salas, D.E., P.J. Salas, and E. Rodriguez-Boulanger. 1987. Modulation of the expression of an apical plasma membrane protein of Madin-Darby canine kidney epithelial cells: cell-cell interactions control the appearance of a novel intracellular storage compartment. *J. Cell Biol.* 104:1249–1259.
- Welchman, D.P., L. Mathies, and J. Ahringer. 2007. Similar requirements for CDC-42 and the PAR-3/PAR-6/PKC-3 complex in diverse cell types. *Dev. Biol.* 305:347–357.
- Wells, C.D., J.P. Fawcett, A. Traweger, Y. Yamanaka, M. Goudreault, K. Elder, S. Kulkarni, G. Gish, C. Virag, C. Lim, et al. 2006. A Rich1/Amot complex regulates the Cdc42 GTPase and apical-polarity proteins in epithelial cells. *Cell*. 125:535–548.
- Wu, X., S. Li, A. Chrostek-Grashoff, A. Czuchra, H. Meyer, P.D. Yurchenco, and C. Brakebusch. 2007. Cdc42 is crucial for the establishment of epithelial polarity during early mammalian development. *Dev. Dyn.* 236:2767–2778.
- Zhang, X., J.W. Cromwell, B.D. Kunjummen, D. Yee, and J. Garcia-Aguilar. 2003. The alpha2 and alpha3 integrins are required for morphologic differentiation of an intestinal epithelial cell line. *Surgery*. 133:429–437.

Supplemental Material

JCB

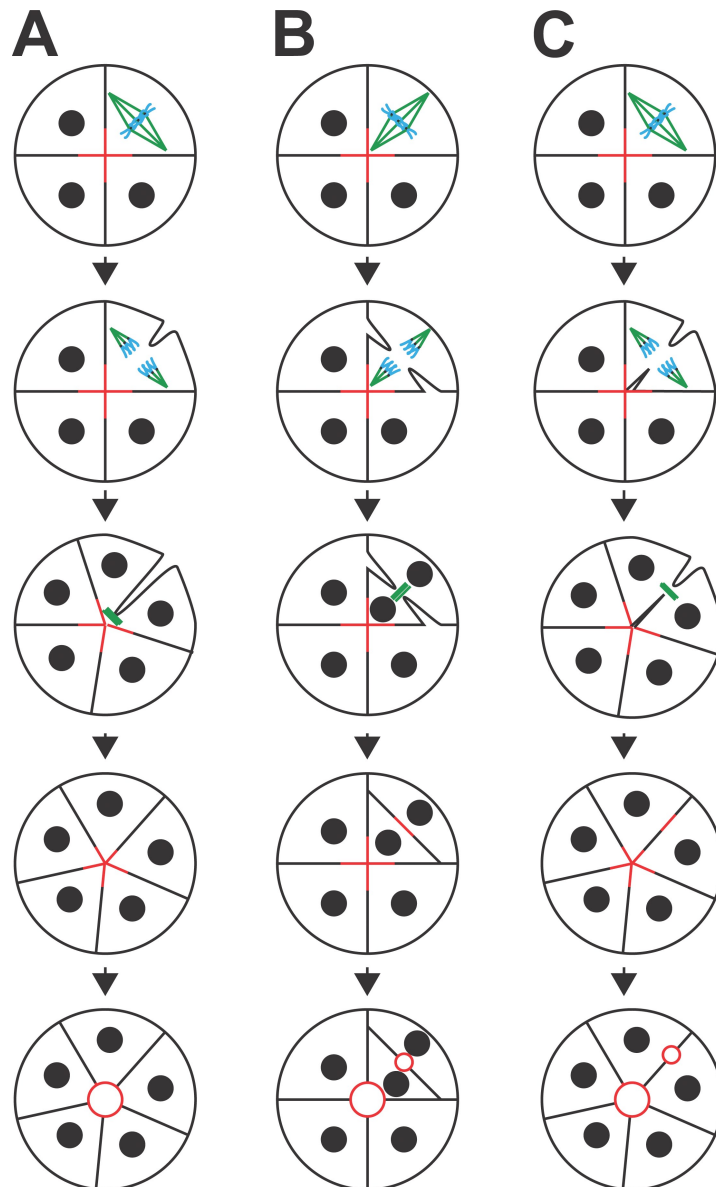
Jaffe et al., <http://www.jcb.org/cgi/content/full/jcb.200807121/DC1>

Figure S1. Spindle orientation and abscission polarity during Caco-2 morphogenesis. (A) Wild-type Caco-2 cystogenesis involves orientated spindles and apically localized abscissions. (B) Loss of spindle orientation would lead to noncentrally localized apical surfaces. (C) Loss of asymmetric abscission could also lead to noncentrally located apical surfaces. Apical membrane, red; spindle and midbody microtubules, green; chromosomes, blue.